J|A|C|S
COMMUNICATIONS

Published on Web 08/29/2008

Insight into the Mechanisms of the Ethylbenzene Disproportionation: Transition State Shape Selectivity on Zeolites

Jun Huang, Yijiao Jiang, V. R. Reddy Marthala, and Michael Hunger*

Institute of Chemical Technology, University of Stuttgart, 70550 Stuttgart, Germany

Received June 24, 2008; E-mail: michael.hunger@itc.uni-stuttgart.de

Chemists and chemical engineers seek to utilize zeolites "under control" in heterogeneously catalyzed reactions.[1] With the ability to finely tune zeolite catalysts by synthesis in a wide range of Si/Al ratios, dealumination, and ion exchange, it is possible to obtain various properties of multiple catalytic sites. Brønsted and Lewis acid sites on zeolites initiate catalytic reactions via proton transfer or hydride abstraction,[2,3] and negatively charged framework oxygen can stabilize formed hydrocarbon cations.[4] These multiple active centers of zeolites can work together to promote a desired reaction. By choosing specific zeolite structures, channel and cage geometry can be varied, which can strongly influence the activity and selectivity in chemical transformations.[4−6] Generally, three mechanisms are described for the shape selective catalysis on zeolites: Reactant shape selectivity, product shape selectivity, and transition state shape selectivity.[1c,d] In contrast to reactant and product shape selectivity, it is difficult to give direct experimental evidence for the transition state shape selectivity. Recently, Clark et al.[7] used theoretical methods to investigate the transition state shape selectivity in the *m*-xylene disproportionation on zeolites. This theoretical study proposed a diphenylmethane-mediated mechanism for FAU-type zeolite catalysts and a methoxide-mediated pathway in more restricted MFI- and MOR-type zeolite catalysts. In the present work, FAU- and MFI-type zeolites with pore sizes of 0.74 and 0.56 nm,[8] respectively, were utilized to examine the transition state shape selectivity in a catalyzed reaction. In addition, these zeolite catalysts have been prepared with suitable catalytic properties, which make the reaction intermediates detectable by solid-state NMR spectroscopy.

Disproportionation of aromatic hydrocarbons is an important petrochemical process.[6,7,9] Ethylbenzene disproportionation has attracted much attention in recent years due to the production of valuable diethylbenzene and as a standard reaction for acidity characterization by the International Zeolite Association (IZA).[9] As shown by earlier studies, this reaction strongly depends on the acidic properties and pore shape of zeolites.[9]

Most of the mechanistic studies of ethylbenzene disproportionation have been carried out in liquid Friedel−Crafts or superacidic catalysts.[10] There are two proposed reaction pathways: (i) the bimolecular diphenylethane-mediated reaction pathway (Scheme 1) and (ii) the monomolecular ethyl-transfer reaction pathway (Scheme 2).[10] Up to now, the reaction intermediates have not been observed. The present study gives experimental evidence for two mechanistic pathways caused by the transition state shape selectivity during the ethylbenzene disproportionation on zeolites. The bulky transition state (diphenylethane species) is directly observed by in situ solid-state NMR spectroscopy on large-pore zeolites upon a "fine-tune" of the acidity (see Supporting Information). However, this intermediate is too large to be formed on medium-pore zeolites ZSM-5, and the ethoxy-mediated pathway was verified for the latter material.

After adsorption of ethyl[α-^{13}C]benzene (**A**) on FAU-type zeolites, the ^{13}C MAS NMR spectra in Figure 1 show a dominating peak at 29 ppm due to the ^{13}C-enriched methylene group of ethylbenzene. Two weak signals at 15 and 129 ppm are assigned to the nonenriched carbon atoms of the methyl group and the aromatic ring, respectively.[11] In contrast to the ^{13}C MAS NMR signal of the enriched methylene group of **A** adsorbed on zeolite H,Na-Y/91 (Figure 1a), these signals are much broader in the spectra of **A** adsorbed on zeolites Al,Na-Y/63 and Al,Na-X/61 (Figure 1b and 1c). Zeolites Al,Na-Y/63 and H,Na-Y were prepared from the same parent material. Lercher and co-workers[3a] reported that 3-fold charged extra-framework lanthanum cations in zeolite X act as strong adsorption sites and can polarize the C−H bonds and even activate alkanes by hydride abstraction under near-ambient conditions. The extra-framework aluminum species of the aluminum-exchanged zeolites X and Y in the present work, therefore, should cause comparable interactions with the side chain of ethylbenzene. These interactions result in a heterogeneity of the adsorbate complexes formed by ethylbenzene and cause a chemical shift distribution responsible for the broadening of the ^{13}C MAS NMR signals of ethyl groups. Quantum chemical calculations indicated that zeolites can initiate the *m*-xylene transalkylation by the hydride

Scheme 1

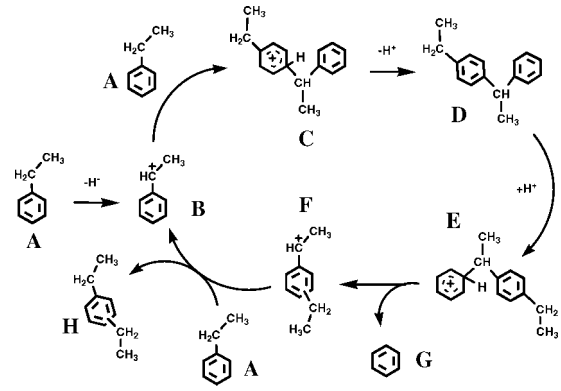

Scheme 2

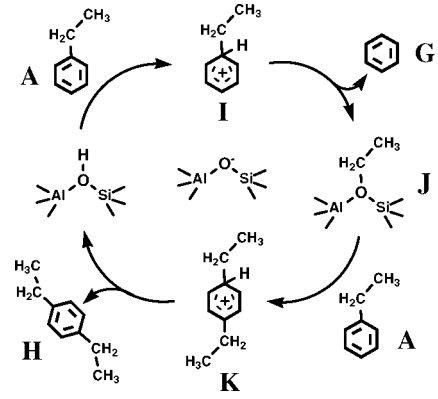

10.1021/ja8042849 CCC: $40.75

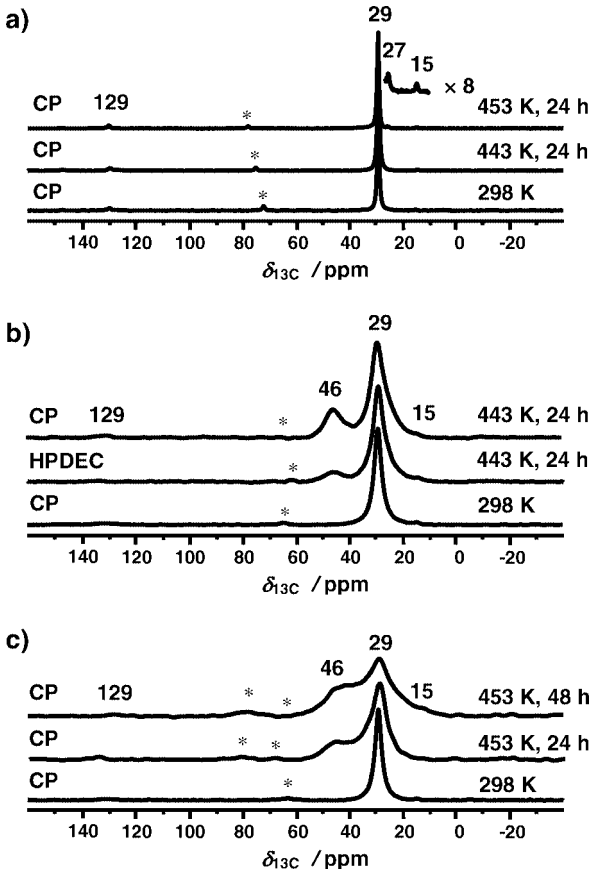

Figure 1. ^{13}C MAS NMR spectra of ethyl[α-^{13}C]benzene conversion on zeolites H,Na-Y/91 (a), Al,Na-Y/63 (b), and Al,Na-X/61 (c). On all these zeolites, two molecules per supercage were loaded. Asterisks indicate spinning sidebands.

abstraction at one of the methyl groups leading to a carbenium ion.[7] In a recent in situ pulsed-flow ^{1}H MAS NMR-UV/vis study, it was shown that extra-framework aluminum species of dealuminated H−Y acting as Lewis acid sites play a crucial role in the formation of sec-ethylphenyl carbenium ions (**B**) by hydride abstraction.[12] The formation of this carbenium ion on zeolite H,Na-Y was found to require higher reaction temperatures or longer heating times.[12]

Upon heating zeolite Al,Na-Y/63 at 443 K for 24 h, a new ^{13}C MAS NMR signal occurred at 46 ppm (Figure 1b), which is due to diphenylethane (**D**). This species was also observed in the ^{13}C CP MAS NMR spectra of ethylbenzene disproportionation on zeolite Al,Na-X/61 at 453 K (Figure 1c). Heating of zeolite H,Na-Y/91 at the same temperatures did not result in a signal of species **D** (Figure 1a), but a signal of diethylbenzene (**H**) appeared at 27 ppm.[11] Benzene (**G**) was generated at the same time. However, it is difficult to be observed in ^{13}C MAS NMR spectra due to its nonenriched ^{13}C atoms. Species **H** should also be produced on zeolites Al,Na-Y/63 and Al,Na-X/61, but this signal might be overlapped by the broad signal at 29 ppm. As described in the Supporting Information, zeolites Al,Na-Y/63 and Al,Na-X/61 were prepared with 11.9 and 16.9 extra-framework aluminum species per unit cell and 2.2 and 1.2 bridging OH groups in the supercages per unit cell, respectively. Furthermore, these materials contain ca. 10.7 and 20.6 SiO$^-$Al/u.c., respectively, acting as base sites.[13] Increasing the number of highly charged Al^{3+} cations can enhance the polarizing effect on the C−H bonds of the methylene group of **A** and the further formation of **B** by hydride abstraction.[3] The hydride ions are stabilized by the extra-framework aluminum cations, and the SiO$^-$Al sites stabilize the nearby **B**. This promotes the reaction of **B** with another **A** to form **C** rather than the recombination with a hydride ion back to **A**. In addition, the SiO$^-$Al sites may stabilize the benzenium-type carbenium ions **C** and **E**, which would contribute to the signal at 46 ppm in Figure 1.

For the transalkylation of *m*-xylene, Clark et al.[7] proposed a direct migration of the additional proton from one aromatic ring to the other in the intermediate diphenylmethane and a subsequent scission. In the present work, this corresponds to a direct step from **C** to **E**, which is split into **F** and **G**. In this case, no formation of **D** would occur in the catalytic cycle. Due to the high energy barriers for the hydride abstraction and transfer (**F** to **B**), the rate of the formation of diphenylethane species would be much lower than that of the scission into **F** and **G**. The diphenylethane species would be rapidly split and could not be the compound observed at 46 ppm in the ^{13}C MAS NMR spectra (Figure 1). Therefore, it must be assumed that the additional proton of **C** migrates to the nearby SiO$^-$Al site leading to species **D**. Due to the small number of Brønsted acid sites in the supercages (0.275 and 0.15 SiOHAl/s.c. for Al,Na-Y/63 and Al,Na-X/61, respectively, with 8 s.c./u.c.), the second aromatic ring of species **D** can not be rapidly protonated to form species **E**. Therefore, species **D** exist with a lifetime that allows observation by ^{13}C MAS NMR spectroscopy (Figure 1b and 1c). In zeolite H,Na-Y/91 with the much higher concentration of Brønsted acid sites of 2.5 SiOHAl/s.c., the species **D** are directly protonated to species **E** on nearby unoccupied Brønsted acid sites and **E** is rapidly split into **F** and **G**. In this case, the short lifetime of **D** makes it undetectable by ^{13}C MAS NMR spectroscopy (Figure 1a). However, the experimental observation of diphenylethane (**D**) in the ethylbenzene disproportionation on zeolites Al,Na-X and Al,Na-Y provides the undoubted evidence that this reaction occurs via the bimolecular reaction pathway on large-pore zeolites (Scheme 1). Because of the significantly smaller pores of zeolite ZSM-5 (0.56 nm) compared to zeolites X and Y (0.74 nm), bulky diphenylmethane-type transition states are too large to be formed on ZSM-5.

Early studies of the alkylbenzene disproportionation in HF−BF_3 solution indicated that the alkyl group maintains its configuration when it transfers from one ring to another via a transition state containing a partial bond between the alkyl group and the second alkylbenzene.[10b] The content of ca. 90% of ethylbenzene was disproportionated via this pathway at room temperature. At higher temperatures (439−553 K), however, the protonated alkylbenzene was split into a benzene molecule and an alkylcarbonium ion. This carbonium ion alkylated a second alkylbenzene to complete the disproportionation or further reacted by polymerization or hydride abstraction. Hence, the alkylbenzene disproportionation by the monomolecular mechanism is accompanied by side reactions leading to complex products.[10b]

Figure 2 shows ^{13}C MAS NMR spectra of ethyl[α-^{13}C]benzene-loaded zeolite Al,Na-ZSM-5 before and after thermal treatments at different temperatures. Before heating, ^{13}C CP MAS signals occur at 15, 29, and 129 ppm, which are assigned to the nonenriched-methyl group, ^{13}C-enriched methylene group, and nonenriched aromatic ring of ethylbenzene, respectively.[11] Upon heating zeolites ZSM-5 at 483 and 503 K for 0.5 h, the reaction starts as indicated by ^{13}C CP MAS NMR signals at 14, 73, and 85−90 ppm. Based on recent studies of the adsorption of ^{13}C-1-ethanol on zeolite H,Na-Y at 453 K, the weak signal at 73 ppm can be assigned to surface ^{13}C-1-ethoxy groups (**J**).[14a] This active surface compound can combine with a second **A** to form diethylbenzene (**H**). Due to the restricted pore size of zeolite ZSM-5, *p*-diethylbenzene is the most preferred product in the disproportionation and only few *m*-diethylbenzenes are formed.[9] The ^{13}C MAS NMR signals of *p*-

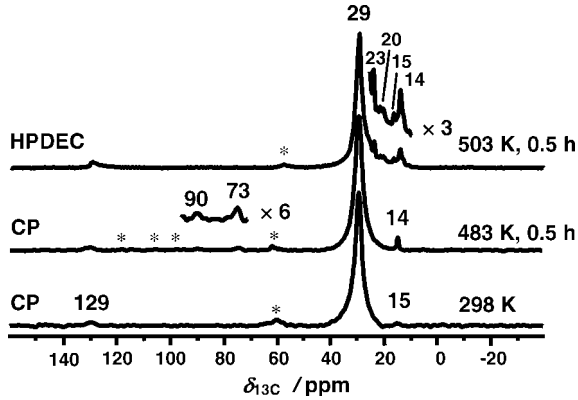

Figure 2. ^{13}C MAS NMR spectra of ethyl[α-^{13}C]benzene conversion on Al,Na-ZSM-5/52 (1 molecule per SiOHAl group). Asterisks indicate spinning sidebands.

and *m*-diethylbenzene occur at 28.8 and 27.9 ppm, respectively.[11] The signals of these products are difficult to distinguish from the strong signal of **A** at 29 ppm.

After decomposition of the surface ^{13}C-1-ethoxy species at 523 K, Wang et al.[14a] observed a weak and broad signal at 78−89 ppm and a strong signal at 13 ppm. Stepanov et al.[14b] detected signals at 89 and 14 ppm after adsorption of ^{13}C-1-ethylene on H-ZSM-5 at 296 K. They assigned the signal at 89 ppm to oligomeric alkoxy groups, which was supported by the signal of terminal methyl carbons of alkoxy groups at 13 to 14 ppm. Accordingly, the signals at 14 and 85−90 ppm in the present work were assigned to terminal methyl carbons of oligomeric alkoxy groups and carbon atoms of these oligomeric alkoxy groups bound to framework oxygen atoms, respectively. Upon thermal treatments of ethylbenzene-loaded zeolites Al,Na-ZSM-5 and H,Na-ZSM-5 at 503 K for 0.5 h and at 573 K for 0.5 or 1 h, respectively, the oligomeric species are further transferred into aromatics (increasing the intensity of peak at 129 ppm), toluene (130, 20 ppm), butane (23 ppm), propane (15), and ethane (6 ppm). These byproducts were also observed upon ethylbenzene disproportionation in the HF−BF_3 solution and are considered as a hint for the monomolecular reaction mechanism.[10b] Therefore, the compared reaction on large-pore zeolites is a clean process without side reactions, which is interesting for industrial applications.

Based on the above-mentioned experimental findings, the ethylbenzene disproportionation on the medium-pore zeolite ZSM-5 is proposed to be a monomolecular reaction via the ethoxy-mediated pathway as summarized in Scheme 2. After adsorption of **A** on ZSM-5, the aromatic ring is rapidly protonated to form the ethylcyclohexadienyl carbenium ion **I** even at room temperature with the low activation energy of 29 kJ/mol.[15] The proton is added to the carbon atom holding the ethyl group to form a σ-complex.[10b] At higher temperatures, the σ-complex **I** is very unstable and splits off an ethyl cation from the aromatic ring to produce the benzene molecule **G**. The alkyl cation is stabilized by a nearby SiO^-Al site and forms a more stable ethoxy group **J**.[7] Subsequently, **J** combines with a second **A** to yield the diethylbenzylium cation with an additional proton at the aromatic ring (**K**). This proton can migrate back to the nearby SiO^-Al site to complete the catalytic cycle, and diethylbenzene **H** is produced as the final product.

In summary, this work provides NMR spectroscopic evidence that the pore shape of zeolite catalysts strongly affects the transition states of ethylbenzene disproportionation and results in different reaction mechanisms. On large-pore zeolites X and Y (ca. 0.74 nm), the bulky diphenylethane species are produced, but this type of transition state is too large to be formed on medium-pore zeolite ZSM-5 (ca. 0.56 nm). The present work shows a bimolecular reaction mechanism of ethylbenzene disproportionation on large-pore zeolites and a monomolecular reaction pathway on medium-pore zeolites via the ethoxy-mediated intermolecular ethyl group transfer. The latter pathway is accompanied by side reactions. Upon "fine-tune" of zeolites X and Y (decrease of Brønsted acid sites, increase of Lewis acid sites and base sites) it is possible to promote the formation of diphenylethane species and reduce their subsequent scission. On these zeolite catalysts, diphenylethane species exist with a lifetime that allows their observation by solid-state NMR spectroscopy.

Acknowledgment. Financial support by the Deutsche Forschungsgemeinschaft is gratefully acknowledged.

Supporting Information Available: Sample preparation and characterization, ethylbenzene disproportionation on H,Na-ZSM-5. This material is available for free of charge via the Internet at http://pubs.acs.org.

References

(1) (a) Rees, L. V. C. *Nature* **1984**, *309*, 583. (b) Hupp, J. T.; Poeppelmeier, K. R. *Science* **2005**, *309*, 2008–2009. (c) Stöcker, M. *Microporous Mesoporous Mater.* **2005**, *82*, 257–292. (d) Smit, B.; Maesen, T. L. M. *Nature* **2008**, *451*, 671–678.
(2) (a) Mildner, T.; Freude, D. *J. Catal.* **1998**, *178*, 309–314. (b) van Santen, R. A.; Kramer, G. J. *Chem. Rev.* **1995**, *95*, 637–660. (c) Corma, A. *Chem. Rev.* **1995**, *95*, 559–614.
(3) (a) Sievers, C.; Onda, A.; Guzman, A.; Otillinger, K. S.; Olindo, R.; Lercher, J. A. *J. Phys. Chem. C* **2007**, *111*, 210–218. (b) Li, S.; Zheng, A.; Su, Y.; Zhang, H.; Chen, L.; Yang, J.; Ye, C.; Deng, F. *J. Am. Chem. Soc.* **2007**, *129*, 11161–11171.
(4) (a) Bhan, A.; Iglesia, E. *Acc. Chem. Res.* **2008**, *41*, 559–567. (b) Farneth, W. E.; Gorte, R. J. *Chem. Rev.* **1995**, *95*, 615–635.
(5) (a) Jones, C. W.; Tsuji, K.; Davis, M. E. *Nature* **1998**, *393*, 52–54. (b) Corma, A.; Fornes, V.; Pergher, S. B.; Maesen, Th. L. M.; Buglass, J. G. *Nature* **1998**, *396*, 353–356. (c) Weisz, P. B.; Haag, W. O.; Rodewald, P. G. *Science* **1979**, *206*, 57–58.
(6) (a) Jones, C. W.; Zones, S. I.; Davis, M. E. *Microporous Mesoporous Mater.* **1999**, *28*, 471–481. (b) Jones, C. W.; Zones, S. I.; Davis, M. E. *Appl. Catal., A* **1999**, *181*, 289–303.
(7) (a) Clark, L. A.; Sierka, M.; Sauer, J. *J. Am. Chem. Soc.* **2004**, *126*, 936–947. (b) Clark, L. A.; Sierka, M.; Sauer, J. *J. Am. Chem. Soc.* **2003**, *125*, 2136–2141.
(8) Meier, W. M.; Olson, D. H.; Baerlocher, Ch. *Atlas of Zeolite Structure Types*, revised 4th ed.; Elsevier: New York, 1996.
(9) (a) De Vos, D. E.; Ernst, S.; Perego, C.; O'Connor, C. T.; Stöcker, M. *Microporous Mesoporous Mater.* **2002**, *56*, 185–192. (b) Weiss, U.; Weihe, M.; Hunger, M.; Karge, H. G.; Weitkamp, J. *Stud. Surf. Sci. Catal.* **1997**, *105*, 973–980. (c) Karge, H. G.; Ernst, S.; Weihe, M.; Weiss, U.; Weitkamp, J. *Stud. Surf. Sci. Catal.* **1994**, *84*, 1807–1812. (d) Arsenova, N.; Bludau, H.; Haag, W. O.; Karge, H. G. *Microporous Mesoporous Mater.* **2000**, *35*−*36*, 113–119. (e) Weihe, M.; Hunger, M.; Breuninger, M.; Karge, H. G.; Weitkamp, J. *J. Catal.* **2001**, *198*, 256–265.
(10) (a) Streitwieser, A.; Reif, L. *J. Am. Chem. Soc.* **1960**, *82*, 5003–5005. (b) McCaulay, D. A.; Lien, A. P. *J. Am. Chem. Soc.* **1953**, *75*, 2411–2413. (c) Lien, A. P.; McCaulay, D. A. *J. Am. Chem. Soc.* **1953**, *75*, 2407–2410.
(11) (a) Philippou, A.; Anderson, M. W. *J. Catal.* **1997**, *167*, 266–272. (b) Pradhan, A. R.; Lin, T.; Chen, W.; Jong, S.; Wu, J.; Chao, K.; Liu, S. *J. Catal.* **1999**, *184*, 29–38.
(12) Huang, J.; Jiang, Y.; Marthala, V. R. R.; Ooi, Y. S.; Hunger, M. *ChemPhysChem* **2008**, *9*, 1107–1109.
(13) Huang, J.; Jiang, Y.; Marthala, V. R. R.; Thomas, B.; Romanova, E.; Hunger, M. *J. Phys. Chem. C* **2008**, *112*, 3811–3818.
(14) (a) Wang, W.; Jiao, J.; Jiang, Y.; Ray, S. S.; Hunger, M. *ChemPhysChem* **2005**, *6*, 1467–1469. (b) Stepanov, A. G.; Luzgin, M. V.; Romannikov, V. N.; Sidelnikov, V. N.; Paukshtis, E. A. *J. Catal.* **1998**, *178*, 466–477.
(15) Huang, J.; Jiang, Y.; Marthala, V. R. R.; Wang, W.; Sulikowski, B.; Hunger, M. *Microporous Mesoporous Mater.* **2007**, *99*, 86–90.

JA8042849